Separation of the magnetic phases at the Néel point in the diluted spin-Peierls magnet $CuGeO_3$

V. N. Glazkov and A. I. Smirnov
P. L. Kapitza Institute for Physical Problems RAS, 117334 Moscow, Russia

K. Uchinokura and T. Masuda
Department of Advanced Materials Science, The University of Tokyo, 7-3-1 Hongo, Bunkyo-ku, Tokyo 113-8656, Japan

(Received 11 May 2001; revised manuscript received 17 September 2001; published 29 March 2002)

The impurity-induced antiferromagnetic ordering of the doped spin-Peierls magnet $Cu_{1-x}Mg_xGeO_3$ was studied by the electron-spin-resonance (ESR) technique. Crystals with $x<4\%$ demonstrate the coexistence of paramagnetic and antiferromagnetic ESR modes. This coexistence indicates the separation of a macroscopically uniform sample in the paramagnetic and antiferromagnetic phases. In the presence of long-range spin-Peierls order (at $x=1.71\%$) the volume of the antiferromagnetic phase immediately below the Néel point T_N is smaller than the volume of the paramagnetic phase. In the presence of the short-range spin-Peierls order ($x=2.88$ and 3.2%) there are comparable volumes of two phases at $T=T_N$. The fraction of the antiferromagnetic phase increases with lowering temperature. In the absence of the spin-Peierls dimerization (at $x=4.57\%$) the whole sample exhibits a transition into an antiferromagnetic state, and there is no phase separation. These results are explained by a consideration of clusters of staggered magnetization appearing near impurities within the singlet spin-Peierls matrix. Overlapping clusters form the antiferromagnetic phase, and isolated clusters contribute to the paramagnetic resonance signal.

DOI: 10.1103/PhysRevB.65.144427 PACS number(s): 75.10.Jm, 75.50.Ee, 76.50.+g

I. INTRODUCTION

The quasi-one-dimensional magnet $CuGeO_3$ is a unique inorganic compound demonstrating a spin-Peierls phase transition.[1] The spin-Peierls transition may occur in a crystal containing spin $S=1/2$ antiferromagnetic chains due to the spin-lattice instability with respect to the dimerization of magnetic ions.[2] Below the transition temperature $T_{SP}=14.5$ K, the lattice period along the chain direction becomes doubled and the exchange integral alternates, taking in turn two values $J\pm\delta J$. Due to this alternation the ground state is a singlet separated from the excited triplet states by an energy gap $\Delta=2$ meV.[3] Thus at low temperatures pure crystals appear to be almost nonmagnetic, and a small residual magnetic susceptibility is provided only by defects. The amplitude of the atomic displacements resulting in the dimerization can be chosen as the order parameter of the spin-Peierls phase. Impurities substituting magnetic or nonmagnetic ions disturb the homogeneity of the spin-Peierls phase in $CuGeO_3$. The doping diminishes the transition temperature and results in an antiferromagnetic long-range ordering.[4–8] The spin-Peierls dimerization and the impurity-induced magnetic order were found to coexist at a low impurity concentration x. The stimulation of the long-range antiferromagnetic order by impurities was explained in Refs. 9–11. The violation of the dimerization around an impurity results in the formation of a solitonlike spin cluster with an antiferromagnetic correlation of neighboring spins and staggered magnetization. The overlapping of clusters and the weak interchain exchange result in the long-range three-dimensional antiferromagnetic order.

The phase transition to the antiferromagnetic state and $T-x$ phase diagram were studied for different types of doping atoms.[12–21] The phase diagram contains areas of a uniform (i.e., without dimerization) paramagnet, of the spin-Peierls states with short- and long-range ordered dimerizations, and of dimerized and uniform antiferromagnetic states. The first-order phase transition between dimerized and uniform antiferromagnetic phases[18,20] takes place in a Mg concentration range between 2.37% and 2.71%. The uniform phase has a higher value of the Néel temperature. The detailed phase diagram is given in Ref. 20. This variety of phases is caused by the competition between the gapped dimerized state and the antiferromagnetic state which is gapless in the exchange approximation. The spin-Peierls state does not allow three-dimensional antiferromagnetic ordering in the pure compound and, on the other hand, impurities restore the antiferromagnetic correlations and suppress the spin-Peierls dimerization.

The goal of this work is an electron-spin-resonance (ESR) study of magnetic properties of different antiferromagnetic phases and of the phase transitions at various phase boundaries of the phase diagram. Previous ESR investigations revealed the multispin nature of clusters formed near impurity ions[22,23] and the gap in the zero-field ESR frequency in the antiferromagnetic phase.[22,24–26] Thus the evolution from isolated clusters with local staggered magnetization to long-range antiferromagnetic order can be followed using the ESR technique. We used single-crystal samples of $Cu_{1-x}Mg_xGeO_3$ from the measurements described in Refs. 18,20 and 21 or samples grown by the same method on the same installation. These samples can be well attributed to the phase diagram presented in Ref. 20. We studied the antiferromagnetic phase transition from dimerized states with long-range spin-Peierls order ($x=1.71\%$) and short-range spin-Peierls order ($x=2.88$, 3.2%), and from the uniform paramagnetic state ($x=4.57\%$).

As a result of this study we found that the formation of antiferromagnetic order at small impurity concentrations is accompanied by a microscopic phase separation into para-

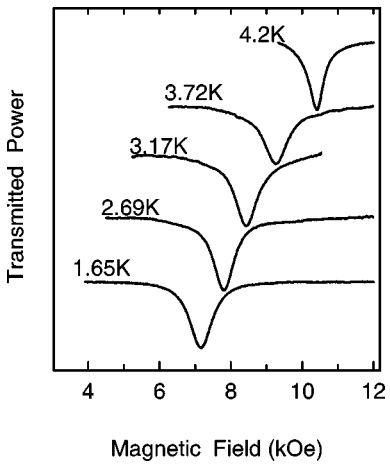

FIG. 1. Evolution of the ESR line for the sample containing 4.57% Mg. $\mathbf{H}\|a$, $f=31$ GHz, and $T_N=4.20$ K.

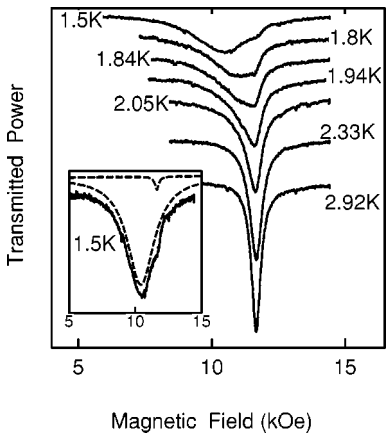

FIG. 2. Evolution of the ESR line for the sample containing 1.71% Mg. $\mathbf{H}\|b$, $f=36$ GHz, and $T_N=2.25$ K. Inset: ESR line at 1.5 K, and the Lorentzian components.

magnetic and antiferromagnetic phases, and that this phase separation differs in temperature evolution for antiferromagnetic phases coexisting with a long- and a short-range ordered spin-Peierls background.

II. EXPERIMENT

Single crystals of $Cu_{1-x}Mg_xGeO_3$ were grown by the floating-zone method. The impurity distribution was checked by the inductively coupled plasma atomic emission spectroscopy technique, and was found to be uniform within 0.1% (see Ref. 20). We used single crystals with dimensions of about $1\times2\times2$ mm^3.

The concentration of residual magnetic defects (both of structural and impurity types) may be estimated from measurements of the ESR intensity of a nominally pure ($x=0$) sample. This intensity rapidly decreases below the transition temperature due to the freezing out of the gapped triplet excitations. The minimum values of the ESR intensity and of the static susceptibility observed at 4.5 K are equal to 5% of these values at T_{SP}. This intensity and susceptibility correspond to the concentration of the residual magnetic defects $x_{def}\sim0.07\%$ per Cu ion.

The ESR spectra were taken by means of a spectrometer with a set of transmission-type resonators. Measurements were carried out in the frequency range 9–75 GHz at temperatures 1.5–15 K. The magnetic resonance absorption line was recorded as a dependence of the transmitted microwave power on the applied magnetic field. The reduction of the transmitted signal is proportional to the microwave power absorbed by the sample.

The temperature evolution of the ESR line for the sample with the impurity concentration $x=4.57\%$ is typical of an antiferromagnet: with a decrease of the temperature starting from the Néel point ($T=T_N$), the single resonance line shifts to lower fields when the magnetic field is perpendicular to the easy axis of the spin ordering (see Fig. 1).

The ESR lines of the samples with $x=1.71\%$ and $x=2.88\%$ are shown in Figs. 2 and 3. At $T=T_N$ the resonance line splits into two spectral components. Similar splitting was observed for the sample with $x=3.20\%$. Below the Néel temperature the ESR line is well described as a sum of two Lorentzian components (see the inset of Fig. 2). The component shifting to lower fields with decreasing temperature has a nonlinear field dependence of the resonance frequency with strong anisotropy, shown in Fig. 4 for the sample with $x=3.20\%$. We note this spectral component as an antiferromagnetic resonance line, since this frequency-field dependence with two gaps is typical for two-axis antiferromagnets.[27] The other spectral component has a linear frequency-field dependence with a temperature-independent g factor. We note this absorption mode as a paramagnetic resonance corresponding to the g-factor values $g_a=2.14$ and $g_b=2.21$ measured for the field orientations along a and b axes correspondingly. These values coincide within the experimental errors with g factors obtained for a pure compound.

The temperature dependence of the resonance fields at a fixed frequency is shown in Fig. 5 for the sample with $x=2.88\%$. The temperature when the low-field line starts to shift from the paramagnetic resonance position corresponds well to the value of T_N obtained by susceptibility

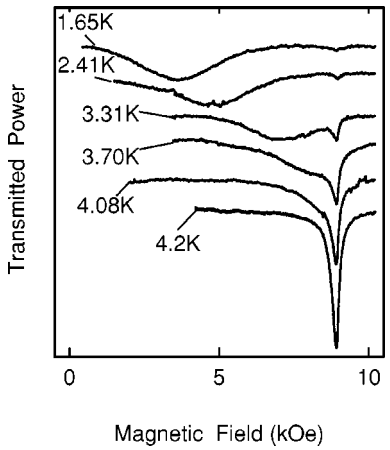

FIG. 3. Evolution of the ESR line for the sample containing 2.88% Mg. $\mathbf{H}\|a$, $f=26.3$ GHz, and $T_N=4.14$ K.

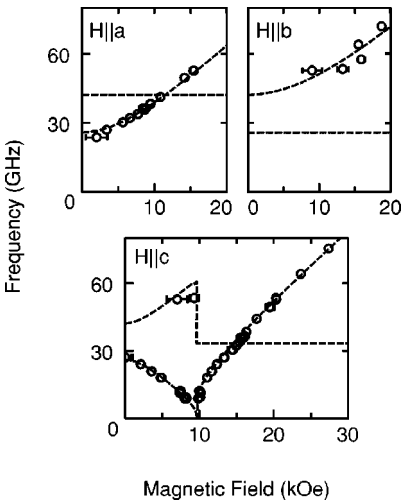

FIG. 4. The spectrum of the antiferromagnetic resonance of the 3.2% Mg-doped sample at $T=1.8$ K for three principal directions of the magnetic field with respect to crystal axes. Dashed lines represent the theoretical calculations following Ref. 27.

measurements.[19,20] There is no difference in ESR spectra taken at cooling and at heating samples, as well no influence of field cooling on the ESR spectra.

To obtain the ESR spectra with two resolvable components, one should take the microwave frequency to be close to the antiferromagnetic resonance gap. In this case the difference between the paramagnetic resonance field and that of a gapped antiferromagnetic resonance mode will be more significant, helping to resolve two spectral components. As shown in Fig. 4, the spectrum of antiferromagnetic resonance of the doped $CuGeO_3$ has two branches with different gaps. The observation of the first or second branch by the field-sweep technique depends on the field orientation. Therefore, to meet the condition mentioned above we selected not only the microwave frequency from the set of the resonant frequencies of the microwave resonator, but also the orientation

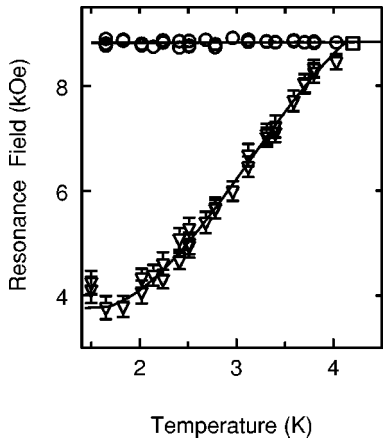

FIG. 5. The temperature dependences of the 26.34-GHz ESR fields for the sample containing 2.88% Mg at $\mathbf{H}\|a$. The sign ∇ corresponds to the antiferromagnetic resonance and the sign $\bigcirc$ to the paramagnetic resonance, $\square$ shows the magnetic resonance above T_N.

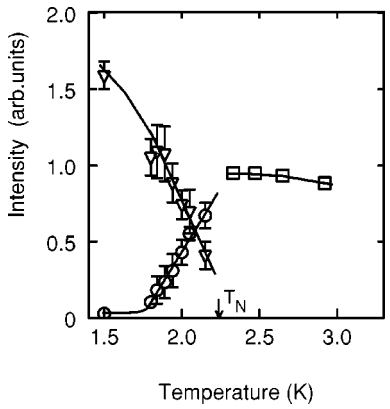

FIG. 6. Temperature dependences of the intensities of the 36-GHz ESR spectral components at $\mathbf{H}\|b$. for a sample with an impurity concentration $x=1.71\%$. The signs $\square$ (above T_N) and ∇ correspond to the antiferromagnetic resonance, and $\bigcirc$ to the paramagnetic resonance below T_N. Solid lines are to guide the eyes.

of the magnetic field with respect to crystal axes. Because the values of gaps also depend on the Mg concentration, data for different samples are obtained at different microwave frequencies and orientations of the external field.

The temperature dependences of the integral intensities of both components are shown in Fig. 6 for $x=1.71\%$, and in Fig. 7 for $x=2.88\%$ and 3.20%. The remarkable feature of the two-component ESR spectrum is the large intensity of the paramagnetic line in a temperature range below the Néel point. For the low concentration $x=1.71\%$, the intensity of the paramagnetic line below the Néel point is close to the integral intensity above T_N, and the intensity of the antiferromagnetic resonance mode is much smaller than that of the paramagnetic mode. For concentrations of $x=2.88\%$ and 3.20% on the contrary, the intensity of the antiferromagnetic resonance is larger than the intensity of the paramagnetic mode. For the concentration $x=4.57\%$ there is no distin-

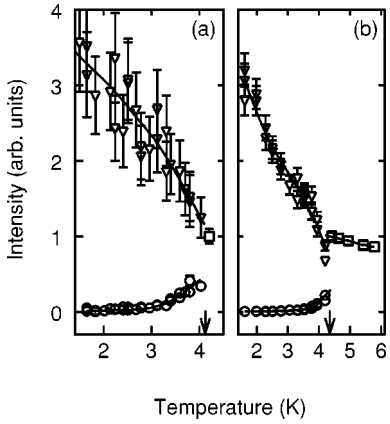

FIG. 7. Temperature dependences of the intensities of spectral components for the samples with impurity concentrations 2.88% (a) and 3.20% (b). The signs $\square$ (above T_N), ∇ and correspond to the antiferromagnetic resonance, and $\bigcirc$ to the paramagnetic resonance below T_N. Solid lines are to guide the eyes. The Néel temperatures are marked by arrows.

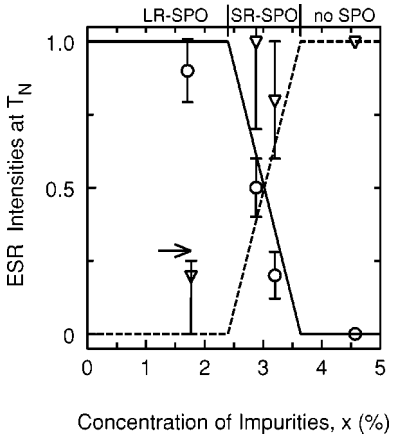

FIG. 8. Relative intensities of antiferromagnetic (▽) and paramagnetic (○) ESR components just below T_N for different concentrations x. Intensities are normalized to the intensity of the paramagnetic mode just above T_N. The lines are linear interpolations between the uniform and long-range spin-Peierls ordering phases. The arrow indicates the volume fraction of interpenetrating spheres at the percolation point according to percolation theory (Ref. 36).

guishable paramagnetic mode below the Néel temperature. We ascribe the entire intensity to the antiferromagnetic mode, and take the intensity of the paramagnetic resonance as zero. The x dependences of the relative intensities of the paramagnetic and antiferromagnetic modes, extrapolated to T_N from low temperatures, are plotted in Fig. 8. Because of significant errors occurring near T_N in the determination of the intensity of a weak and wide antiferromagnetic component near the narrow paramagnetic line, the intensity of the antiferromagnetic component tends to be overestimated.

III. DISCUSSION

A. Phase separation

In a typical antiferromagnet it is expected that only antiferromagnetic resonance modes will be present below the Néel point. This behavior is confirmed in numerous experiments on the antiferromagnetic resonance. We observe the expected single-mode ESR only in the $x=4.57\%$ sample. At lower concentrations, however, antiferromagnetic and paramagnetic modes coexist. The extra paramagnetic mode could originate (i) from isolated Cu ions located at the surface or at structure defects; (ii) from triplet excitations of the spin-Peierls matrix, which are present both in pure and doped crystals[7,15,28]; or (iii) from the nonuniform distribution of the impurities resulting in a smeared transition to the antiferromagnetic state.

The first proposition may be excluded, because the intensity of the signal we observe diminishes with temperature, while the ESR intensity of the isolated defects should demonstrate a Curie-like increase of intensity. The second suggestion should also be declined, because the paramagnetic resonance signal at $T<T_N$ is too intensive to be attributed to triplet excitations. At our microwave frequencies, which are an order of magnitude smaller than the spin-gap frequency $\Delta/\hbar$, the ESR intensity of triplet excitations decreases strongly with cooling,[29,30] in the same manner as the dc susceptibility. The triplet contributions at $x=1.71\%$ and $x=0$ should be approximately equal, because the values of T_{SP} for these concentrations are close. The ESR absorption of $x=0$ samples gives an upper estimate for the triplet contribution, since this absorption contains, in addition, a Curie-like part due to residual defects. The ESR intensity of the pure sample has a minimum at 5 K. At this temperature the ESR intensity of the pure sample is an order of magnitude smaller than the intensity of the paramagnetic resonance mode of the $x=1.71\%$ sample at $T=2$ K. Upon lowering the temperature the triplet contribution continues to decrease; therefore, the triplet part of the ESR intensity in the doped sample is at least an order of magnitude smaller than the intensity of the paramagnetic resonance mode observed below $T_N=2.5$ K. To derive the triplet contribution in a more accurate manner, we followed the procedure described in Ref. 16. This procedure uses an interpolating formula for triplet susceptibility, accounting for the dependence of the gap on the temperature and impurity concentrations, and is adequate for low-doped samples in the paramagnetic phase. Following this method, at 5 K we obtain an estimation of the triplet contribution for $x=1.71\%$ to about 10^{-3} of the observed intensity. Extrapolating the temperature dependence for the triplet susceptibility to lower temperatures, we obtain even smaller values, and thus surely exclude the triplet states as the source of the paramagnetic resonance signal in the antiferromagnetic phase.

Finally, the third explanation, based on the trivial inhomogeneous distribution of the Mg concentration, is also invalid because the distribution of the Néel temperature should result in a wide band of absorption, while the observed antiferromagnetic resonance absorption is well described by a single Lorentzian. In addition the range of the distribution of x which is necessary to account for the paramagnetic phase is much wider than what is obtained in measurements. For example, to have the Néel points in the range 1.5–2.25 K, where both signals are present for the $x=1.71\%$ sample, we should imagine a concentration distribution in the range 1.3–2.2 %. The width of this range is much larger than the measured value of 0.1%. The well-defined singularities in the temperature dependences of the susceptibility[20] and the resonance field (see Fig. 5) prove that the samples are macroscopically uniform. The width of the transition to the Néel state may be estimated from the susceptibility and ESR data, and is not larger than 0.1 K.

Summarizing the above analysis of possible sources for the paramagnetic resonance mode below the Néel point, we state that the observed paramagnetic resonance signal cannot be ascribed to the sources enumerated above. This signal should be due to the same spin system of Cu^{2+} ions as the whole spin-Peierls matrix, but not to triplet excitations of that matrix. It is difficult to explain this signal as originating from a homogeneous spin system; therefore, we assume that the two ESR modes are due to the separation of the sample into paramagnetic and antiferromagnetic phases.

Note that the paramagnetic resonance line remains at the same magnetic field while the antiferromagnetic resonance line demonstrates a strong shift at lowering temperature. This

fact indicates the absence of any coupling between the spins, oscillating on two close frequencies, because coupled spins are known to change their eigenfrequencies simultaneously when changing an external parameter (see, e.g. Refs. 31 and 32). This argument proves the phase separation, because ESR signals coming from the same places in the Cu spin system should be coupled, and should demonstrate simultaneous shifts of both frequencies.

B. Model

To explain the microscopic phase separation at low impurity concentrations, when long-range dimerization order occurs, we consider the regions of staggered magnetization[9,10] (spin clusters) appearing near impurity atoms. The spins within these clusters have nonzero average spin projections; therefore, the local Néel order parameter can be introduced. In addition a cluster has a net magnetic moment equal to μ_B. The formation of clusters is confirmed in calculations of the staggered magnetization near the ends of spin chain segments in a spin-Peierls magnet [see, e.g., Fig. 2(b) of Ref. 9, demonstrating the appearance of the staggered magnetization on rather long chain parts near the ends of segments]. The correlation length along the spin chain ξ_c is estimated to be of about ten interspin distances.[10,33] The interchain exchange integrals should result in spin-spin correlations transverse to the chain direction. The transverse correlation lengths $\xi_{a,b}$ may be estimated analogous to the estimation of the longitudinal correlation length[34,35] as follows: $\xi_i \sim v_i/\Delta$, here $v_i \sim J_i l_i$ is the spinon velocity, with J_i being the interchain exchange integrals along the directions a and b; l_i are the lattice constants along these transverse directions. Thus the cluster at $T=0$ may be considered as a three-dimensional (3D) region with staggered magnetization located near the impurity and with an exponential decay of this staggered magnetization when moving away from the impurity. At finite temperature the coherence of the antiferromagnetic order parameter which is spatially variable on the wing of the cluster will be destroyed by thermal fluctuations. The distance L in the chain direction of the region of the coherent antiferromagnetic order parameter may be estimated from the relation

$$k_B T = JS^2 \exp\{-2L/\xi_c\}. \tag{1}$$

The distances of the coherence along transverse directions are taken to be equal to $(\xi_i/\xi_c)L$. For crude modeling we consider the area of the spatially coherent antiferromagnetic order at finite temperature as a 3D antiferromagnetic drop of the ellipsoidal form with fixed boundaries. This drop is elongated along the spin chain direction, and the ratio of the drop dimensions along and transverse to the chain is of about the ratio of corresponding exchange integrals. For $CuGeO_3$ we have this ratio according to Refs. 3 and 35: $J_b/J=0.11$ and $|J_a|/J=0.011$.

The size of an ellipsoidal drop enlarges when temperature is lowered according to relation (1). The drops are placed in space at random, with the density of the drops corresponding to the value of the concentration of impurities. The antiferromagnetic order parameter is nonzero within ellipsoids and zero outside them. The 2D illustrative model is shown in Fig. 9. The concentration value 0.1% is chosen because this low value enables us to follow step by step the process of the formation of the ordered phase. At a concentration of about 1% the picture remains qualitatively the same. At high temperatures, when the drops are small and do not overlap [Fig. 9(a)], the phases of the local order parameters of different drops are not coherent, and the model shows no long-range antiferromagnetic order. Clusters contribute to the static susceptibility and the ESR signal due to their net magnetic moments equal to μ_B, giving rise to a Curie-like susceptibility and a paramagnetic resonance signal. Upon lowering the temperature the drops grow and begin to overlap [Fig. 9(b)]. The order parameter in the overlapped drops (a conglomerate of drops) is coherent; thus large areas with coherent antiferromagnetic ordering appear. For large conglomerates the antiferromagnetic susceptibility prevails over the paramagnetic susceptibility, which is due to a magnetic moment of only one spin. At this point the susceptibility measurement should detect the antiferromagnetic transition and the appearance of an antiferromagnetic resonance signal. The order parameter percolates through the macroscopic distance [Fig. 9(c)] as in the known problem of percolation through interpenetrating spheres placed at random. The theory[36] predicts a percolation point in 3D space at the critical value of the volume fraction occupied by spheres equal to 0.286. At the phase transition (at the percolation point) there is a phase separation: there are intersecting threads of an antiferromagnetically ordered phase [marked with black color on Fig. 9(c)], and a paramagnetic phase consisting of a dimerized spin-Peierls matrix (white) and still remaining isolated drops (gray). We should observe both an antiferromagnetic resonance signal from the

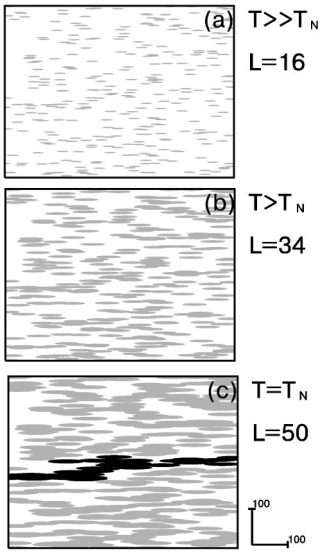

FIG. 9. Illustration of the two-dimensional modeling of the formation of the long-range antiferromagnetic order. Spin chains are directed horizontally, drops of the correlated spins are shown by gray filling, the spin-Peierls matrix by white filling, and the macroscopic group of drops is marked by black filling. The scale is given in interspin distances. The modeling is performed for $x=0.1\%$ and the following values of L (in interspin distances): (a)$L=16$, (b)$L=34$, and (c)$L=50$.

ordered phase and a paramagnetic resonance signal from the small drops isolated within the dimerized matrix.

As the temperature decreases further, the isolated drops join the antiferromagnetic phase and the volume of the ordered phase increases. The volume of the paramagnetic phase reduces, and the intensity of the paramagnetic signal should diminish with the temperature decrease. The scenario described above mainly explains the observed phase separation and the experimental data in the low concentration limit. The dimerized singlet background and the random distribution of impurities are of importance for this scenario.

For the paramagnetic state the integral intensity of absorption is proportional to the static susceptibility. The integral intensity of the antiferromagnetic modes should be proportional to the susceptibility of the antiferromagnet but with another coefficient (see, e.g. Ref. 37). Thus the ratio of the intensity of paramagnetic component just below the Néel temperature to the intensity of the ESR line above the Néel temperature is a measure of the sample volume occupied by the paramagnetic phase. The ratio of the antiferromagnetic component intensity to the ESR intensity above T_N represents only qualitatively the fraction of the antiferromagnetic phase (the ratio of coefficients is of the order of unity). We can also estimate the volume of the antiferromagnetic fraction as the sample volume which is not occupied by the paramagnetic phase. The values of the ESR intensity normalized to the intensity above the Néel point for different samples are presented on Fig. 8. The antiferromagnetic fraction just below T_N, obtained by both ways, is small (between zero and 25% of the sample volume) for the sample with $x=1.71\%$. For the samples with $x=2.88\%$ and 3.2% this fraction is larger, and exceeds half of the sample volume, and for $x=4.57\%$ the whole sample becomes antiferromagnetic at the Néel point. As mentioned in Sec. I these concentrations correspond to two different kinds of spin-Peierls order and to the absence of spin-Peierls order. Taking this into account, we deduce that (i) the volume of the antiferromagnetic phase at $T=T_N$ is small when the ordering takes place at the long-range spin-Peierls order; (ii) at short-range spin-Peierls order there are comparable volumes of two phases at the $T=T_N$; and (iii) in the absence of spin-Peierls dimerization the whole sample becomes ordered at the transition temperature. The first conclusion is in agreement with the model described above: the volume of a percolating thread is smaller than the sample volume [see Fig. 9(c)]. The estimation of the antiferromagnetic fraction of about 25% is in a qualitative agreement with the result of the percolation theory, and hence with the constructed model.

We cannot extrapolate the constructed model to a situation with short-range dimerization order. Nevertheless it is natural to propose that in the corresponding concentration range, the behavior of the system should be intermediate between the behaviors of dimerized and uniform crystals with defects. This proposition is shown in Fig. 8 by straight lines, interpolating the fraction of the antiferromagnetic phase from a small value at long range spin-Peierls order to unity at an undimerized phase. This hypothesis is in a qualitative agreement with our observations. Further detailed investigations of the amount of the ordered phase just below the Néel point for different concentration would by of great interest.

It is worth noting that in several previous investigations of the antiferromagnetic phase in doped $CuGeO_3$ a two-component signal was not observed.[22,24,26] The single line may be explained here either by frequencies far from the antiferromagnetic resonance gaps[26] or by large impurity concentrations which suppress the dimerization.[22,24] A two-component line, with spectra and temperature dependence analogs to those reported in the present work was observed in experiments with $Cu_{0.98}Zn_{0.02}GeO_3$.[25]

IV. CONCLUSION

ESR measurements reveal the microscopic phase separation at the impurity induced antiferromagnetic ordering in the spin-Peierls magnet $CuGeO_3$. The temperature evolution of an ordered phase volume with a small volume fraction at the Néel point indicates the percolating character of the antiferromagnetic phase transition at a low doping level when the antiferromagnetic and spin-Peierls order coexist.

ACKNOWLEDGMENTS

The authors are indebted to S. S. Sosin for valuable discussions. This work was supported by a joint grant from the Russian Foundation for Basic Research and Deutsche Forschung Gesellschaft (Project No. 01-02-04007), by INTAS Project No. 99-0155, and by Award No. RP1-2097 from the U.S. Civilian Research and Development Foundation for the Independent States of the former Soviet Union (CRDF). One of the authors (V.G.) thanks Forshungscentrum Julich Gmbh for continuous support of his work.

[1] M. Hase, I. Terasaki, and K. Uchinokura, Phys. Rev. Lett. **70**, 3651 (1993).

[2] E. Pytte, Phys. Rev. B **10**, 4637 (1974).

[3] M. Nishi, O. Fujita, and J. Akimitsu, Phys. Rev. B **50**, 6508 (1994).

[4] M. Hase, I. Terasaki, Y. Sasago, K. Uchinokura, and H. Obara, Phys. Rev. Lett. **71**, 4059 (1993).

[5] M. Hase, N. Koide, K. Manabe, Y. Sasago, and K. Uchinokura, Physica B **215**, 164 (1995).

[6] S.B. Oseroff, S. -W. Cheong, B. Aktas, M.F. Hundley, Z. Fisk, and L.W. Rupp, Jr., Phys. Rev. Lett. **74**, 1450 (1995).

[7] L.P. Regnault, J.P. Renard, G. Dhalenne, and A. Revcolevschi, Europhys. Lett. **32**, 579 (1995).

[8] J.-G. Lussier, S.M. Coad, D.F. McMorrow, and D.McK. Paul, J. Phys.: Condens. Matter **7**, L325 (1995).

[9] H. Fukuyama, T. Tanimoto, and M. Saito, J. Phys. Soc. Jpn. **65**, 1182 (1996).

[10] D. Khomskii, W. Geertsma, and M. Mostovoy, Czech. J. Phys. **46**

S6, 3239 (1996).
[11] M. Mostovoy, D. Khomskii, and J. Knoester, Phys. Rev. B **58**, 8190 (1998).
[12] J.-P. Renard, K. Le Dang, P. Veillet, G. Dhalenne, A. Revcolevschi, and L.-P. Regnault, Europhys. Lett. **30**, 475 (1995).
[13] M. Hase, K. Uchinokura, R.J. Birgenau, K. Hirota, and G. Shirane, J. Phys. Soc. Jpn. **65**, 1392 (1996).
[14] S. Coad, J.-G. Lussier, D.F. McMorrow, and D. McK. Paul, J. Phys.: Condens. Matter **8**, 6251 (1996).
[15] M.C. Martin, M. Hase, K. Hirota, G. Shirane, Y. Sasago, N. Koide, and K. Uchinokura, Phys. Rev. B **56**, 3173 (1997).
[16] B. Grenier, J.-P. Renard, P. Veillet, C. Paulsen, G. Dhalenne, and A. Revcolevschi, Phys. Rev. B **58**, 8202 (1998).
[17] K. Manabe, H. Ishimoto, N. Koide, Y. Sasago, and K. Uchinokura, Phys. Rev. B **58**, R575 (1998).
[18] T. Masuda, A. Fujioka, Y. Uchiyama, I. Tsukada, and K. Uchinokura, Phys. Rev. Lett. **80**, 4566 (1998).
[19] H. Nakao, M. Nishi, Y. Fujii, T. Masuda, I. Tsukada, K. Uchinokura, K. Hirota, and G. Shirane, J. Phys. Soc. Jpn. **68**, 3662 (1999).
[20] T. Masuda, I. Tsukada, K. Uchinokura, Y.J. Wang, V. Kiryukhin, and R.J. Birgeneau, Phys. Rev. B **61**, 4103 (2000).
[21] V. Kiryukhin, Y.J. Wang, S.C. LaMarra, R.J. Birgeneau, T. Masuda, I. Tsukada, and K. Uchinokura, Phys. Rev. B **61**, 9527 (2000).
[22] V.N. Glazkov, A.I. Smirnov, O.A. Petrenko, D.McK. Paul, A.G. Vetkin, and R.M. Eremina, J. Phys.: Condens. Matter **10**, 7879 (1998).
[23] V.N. Glazkov, A.I. Smirnov, G. Dhalenne, and A. Revcolevschi, Zh. Éksp. Teor. Fiz **120**, 164 (2001) [JETP **93**, 143 (2001)].
[24] M. Hase, M. Hagiwara, and K. Katsumata, Phys. Rev. B **54**, R3722 (1996).
[25] A.I. Smirnov, V.N. Glazkov, A.N. Vasil'ev, L.I. Leonyuk, S.M. Coad, D.McK. Paul, G. Dhalenne, and A. Revcolevschi, Pisma Zh. Éksp. Teor. Fiz. **64**, 277 (1996) [JETP Lett. **64**, 305 (1996)].
[26] H. Nojiri, T. Hamamoto, Z.J. Wang, S. Mitsudo, M. Motokawa, S. Kimura, H. Ohta, A. Ogiwara, O. Fujita, and J. Akimitsu, J. Phys.: Condens. Matter **9**, 1331 (1997).
[27] T. Nagamiya, K. Yosida, and R. Kubo, Adv. Phys. **4**, 1 (1955).
[28] Y. Sasago, N. Koide, K. Uchinokura, M.C. Martin, M. Hase, K. Hirota, and G. Shirane, Phys. Rev. B **54**, R6835 (1996).
[29] M. Honda, T. Shibata, K. Kindo, Sh. Sugai, T. Takeuchi, and H. Hori, J. Phys. Soc. Jpn. **65**, 691 (1996).
[30] S. Oseroff, S.-W. Cheong, A. Fondado, B. Aktas, and Z. Fisk, J. Appl. Phys. **75**, 6819 (1994).
[31] P.W. Anderson, J. Phys. Soc. Jpn. **9**, 316 (1954).
[32] D.B. Chesnut and W.D. Philips, J. Chem. Phys. **35**, 1002 (1961).
[33] K.M. Kojima, Y. Fudamoto, M. Larkin, G.M. Luke, J. Merrin, B. Nachumi, Y.J. Uemura, M. Hase, Y. Sasago, K. Uchinokura, Y. Ajiro, A. Revcolevschi, and J.-P. Renard, Phys. Rev. Lett. **79**, 503 (1997).
[34] K. Okamoto, J. Phys. Soc. Jpn. **56**, 912 (1987).
[35] L.-P. Regnault, M. Aïn, B. Hennion, G. Dhalenne, and A. Revcolevschi, Phys. Rev. B **53**, 5579 (1996).
[36] V.K.S. Shante and S. Kirkpatrick, Adv. Phys. **20**, 325 (1971).
[37] E. A. Turov, *Physical Properties of Magnetically Ordered Crystals* (Academic Press, New York, 1965), Chap. 9, Sec. 2.